

Optical bistability and phase transitions in a doped photonic band-gap material

Sajeev John and Tran Quang

Department of Physics, University of Toronto, 60 St. George Street, Toronto, Ontario, Canada M5S 1A7

(Received 29 March 1996)

We discuss the nonlinear response of impurity two-level atoms in a pseudophotonic band gap (PBG) to an applied laser field. It is shown that in the case when the variance of resonant dipole-dipole interaction (RDDI) is much larger than its average value and the spontaneous emission rate, a nonequilibrium second-order phase transition occurs when the applied field strength parameter exceeds the variance of RDDI. This situation arises when the atomic density is low and the resonance frequency is near the center of a wide PBG. At this threshold the system changes from glassy phase to ferroelectric phase. In the case when the average value of RDDI is larger than its variance and spontaneous emission decay rate, this phase transition becomes first order, leading to optical bistability. This situation arises when the atomic density is high or when the photon localization length within the PBG extends over many optical wavelengths. The influence of RDDI fluctuation on bistability is discussed. These results suggest that disordered, impurity-doped, PBG materials may exhibit very low threshold switching properties. [S1050-2947(96)02111-7]

PACS number(s): 42.65.An, 42.50.Fx, 42.65.Pc

I. INTRODUCTION

The concepts of photon localization [1] and photonic band gaps (PBG's) [2,3] have provided the basis for a new research direction of potential technological importance [4–6]. Since the initial fabrication [5] of a three-dimensional PBG structure in the microwave regime, considerable effort has been concentrated on designing and microfabricating PBG structures in the near-infrared and visible frequency regimes. The original three-cylinder structure of Yablonovitch, Gmitter, and Leung [5] has been reproduced in the visible spectrum using reactive ion etching techniques. The relative difficulty in drilling to a depth of more than a few unit cells of the periodic structure in the visible spectrum has spurred other researchers to design alternative structures more amenable to layer-by-layer microfabrication using well-known chemical etching techniques [6]. Most notable of these is the structure constructed by Ozbay *et al.* [7] and the so-called A-7 structures proposed by Chan *et al.* [8]. These consist of stacked wafers of either GaAs, Si, or alumina, grown layer by layer and chemically etched to produce a three-dimensional periodic structures with the point group symmetry of a diamond lattice. Photonic band gaps as large as 30% of the center frequency have been demonstrated in such structures. Photonic crystals using silicon wafers have been fabricated for wavelengths approaching $600 \mu\text{m}$ using these concepts. The ultimate goal is to design and fabricate photonic crystals for use at $1.5 \mu\text{m}$, the canonical wavelength used in the optoelectronics industry. Recently, Fan *et al.* [9] have designed a class of photonic crystals for fabrication at sub-micrometer length scales using Si and SiO_2 layers. These structures involve layered growth, followed by selective chemical etching of the two dielectric materials, followed in turn by the etching of long cylindrical holes from the top surface of the sample. This approach may soon lead to large scale PBG microstructures in the visible and near-visible wavelength regimes. We mention finally the striking discovery of certain self-organizing periodic dielectrics in the near infrared. Gruning, Lehmann, and Engelhardt [10] have fab-

ricated a very large scale two-dimensional PBG structure using macroporous silicon. Using the appropriate electrochemical etching methods, these researches have shown that a highly ordered array of macropores can be induced to form even without recourse to methodical layer-by-layer growth. The recent progress, described above, in microfabrication of PBG materials further motivates our theoretical study of this new field which crosses the boundary between quantum optics and solid state physics.

Photonic band-gap materials constitute a fundamentally new class of dielectric materials in which the basic electromagnetic interaction is controllably altered. It has been suggested that this would be accompanied by the inhibition of spontaneous emission and fractionalized single atom inversion [1,11], photon localization [3,12], photon hopping conduction [13], vacuum Rabi splitting, and photon-atom bound states [14]. Numerous applications of PBG materials have been discussed in Refs. [12,15,16]. These include zero-threshold, high efficiency microlasers, as well as high modulation speed laser systems which operate even in the absence of a cavity mode [12]. One of the key points which distinguishes quantum electrodynamics (QED) in a PBG from QED in free space is that in addition to suppression of spontaneous emission, certain coherent propagation effects can be selectively preserved. In particular, when an atomic transition lies deep inside the gap, the spontaneous emission is strongly suppressed whereas coherent dipole-dipole interaction between identical atoms persists on a length scale given by the localization length of the dielectric microstructure [14,17] as a result of the exchange of high-energy virtual photons between atoms. This leads to coherent processes such as photon hopping conduction [13] and the formation of a quantum-optical spin-glass state accompanied by a Bose-glass state of photons in the localized cavity mode [18].

In this paper we investigate nonequilibrium phase transitions and bistability in the nonlinear response of impurity two-level atoms in an imperfect PBG to an applied laser field. The atomic resonance frequency is assumed to lie sufficiently far from the band edge that non-Markovian effects

caused by irregularity of the density of modes at the band edge can be ignored. We show that when the variance of resonant dipole-dipole interaction (RDDI), J , is much larger than its average value J_0 and the atomic population decay $1/T_1$ rate as well as the rate of dipole dephasing $1/T_2$, a second-order nonequilibrium phase transition occurs at a specific threshold intensity of the applied field. The value of this threshold intensity is controlled by the parameter J . At this threshold the system changes from a glassy phase into a ferroelectric phase. In the opposite case in which the average value J_0 is larger than J and $1/T_2$, this nonequilibrium transition is first order, leading to optical bistability. This is similar in some respects to intrinsic optical bistability of a dense medium in free space, described in numerous papers [19,20]. The difference here is that the decay times T_1 and T_2 can be very large in a PBG and as a result the optical bistability may occur at very low intensity of an applied field and the required density of atoms is relatively small. This suggests that bistable PBG materials may act as very low threshold switches and amplifiers in integrated optical circuits. The influence of fluctuations of RDDI on bistability is discussed in detail.

II. THE BASIC EQUATIONS

We study the response to an applied field of two-level atoms placed within a PBG material with a pseudogap of localized states. This pseudogap consists of surface-localized modes, localized defect modes in the interior of the photonic crystal, and in certain cases [21], isolated propagating modes along specific symmetry direction of the periodic microstructure.

The Hamiltonian which describes the system in the rotating-wave and the electric dipole approximation is given by (in the interaction picture)

$$\begin{aligned}
H = & \hbar \sum_{\lambda} \delta_{\lambda} a_{\lambda}^{\dagger} a_{\lambda} - \frac{\hbar}{2} \delta \sum_i \sigma_i^z \\
& - i \hbar \sum_{\lambda, i} g_{\lambda i} (a_{\lambda}^{\dagger} \sigma_i e^{-i\vec{k} \cdot \vec{r}_i} - \sigma_i^{\dagger} a_{\lambda} e^{i\vec{k} \cdot \vec{r}_i}) \\
& - \hbar \sum_i \Omega (\sigma_i e^{-i\vec{k}_0 \cdot \vec{r}_i} + \sigma_i^{\dagger} e^{i\vec{k}_0 \cdot \vec{r}_i}). \quad (1)
\end{aligned}$$

Here, σ_i^{\dagger} and σ_i describe atomic excitation and deexcitation of the i th atom with coordinates \vec{r}_i , respectively; σ^z describes the atomic inversion; a_{λ} and a_{λ}^{\dagger} are the radiation field annihilation and creation operators for photons of the allowed modes ($\lambda \equiv \vec{k}, \vec{e}_{\lambda}$ where \vec{e}_{λ} are the two transverse unit polarization operators); $\delta = \omega - \omega_a$ and $\delta_{\lambda} = \omega_{\lambda} - \omega_a$ where ω_a , ω , and ω_{λ} are the atomic resonant frequency, the applied field frequency, and the frequency of a mode λ , respectively; \vec{k}_0 and \vec{k} are the wave vectors of the applied field and of the radiation mode λ ; and $g_{\lambda i}$ is the atomic field coupling constant

$$g_{\lambda i} = \frac{\omega_a \mu}{\hbar} \left(\frac{\hbar}{2 \epsilon_0 \omega_{\lambda} V} \right)^{1/2} \vec{e}_{\lambda} \cdot \vec{u}_i. \quad (2)$$

Here \vec{u}_i and μ are the unit vector and the absolute values of the dipole moment of the i th atom, V is the sample volume, and ϵ_0 is the Coulomb constant. $\Omega = \mu E / \hbar$ is the resonant Rabi frequency where E is the amplitude of the applied field. The general (non-Markov) Bloch equations, resulting from the Hamiltonian (1), are derived in Appendix A. Here, we focus only on the case when the atomic resonant frequency lies deep in the pseudogap where the density of modes does not change considerably over the immediate surrounding spectral regions. In such a case, non-Markov effects caused by the irregularity in the density of states at the edges of a PBG can be ignored [13,18,22] and the Bloch equations (A5) and (A6) simplify to

$$\begin{aligned}
\frac{d}{dt} \langle \sigma_i \rangle = & (i \delta + i \delta_L - 1/T_2) \langle \sigma_i \rangle - i \Omega e^{i\vec{k}_0 \cdot \vec{r}_i} \langle \sigma_i^z \rangle \\
& + \sum_{j(\neq i)} \gamma_{ij} \langle \sigma_i^z \sigma_j \rangle + i \sum_{j(\neq i)} J_{ij} \langle \sigma_i^z \sigma_j \rangle, \quad (3)
\end{aligned}$$

$$\begin{aligned}
\frac{d}{dt} \langle \sigma_i^z \rangle = & - (\langle \sigma_i^z \rangle + 1) / T_1 + 2i \Omega (\langle \sigma_i^+ \rangle e^{i\vec{k}_0 \cdot \vec{r}_i} - \langle \sigma_i \rangle e^{-i\vec{k}_0 \cdot \vec{r}_i}) \\
& - 2 \sum_{j(\neq i)} [\gamma_{ij} \langle \sigma_i^+ \sigma_j + \sigma_j^+ \sigma_i \rangle \\
& + i J_{ij} \langle \sigma_i^+ \sigma_j - \sigma_j^+ \sigma_i \rangle]. \quad (4)
\end{aligned}$$

Here

$$1/T_2 = 1/(2T_1) = \pi \sum_{\lambda} g_{\lambda i}^2 \delta(\omega_{\lambda} - \omega_a), \quad (5)$$

$$\delta_L = \sum_{\lambda} g_{\lambda i}^2 \text{P} \left(\frac{1}{\omega_{\lambda} - \omega_a} \right), \quad (6)$$

$$\gamma_{ij} = \pi \sum_{\lambda} g_{\lambda i} g_{\lambda j} e^{i\vec{k} \cdot \vec{r}_{ij}} \delta(\omega_{\lambda} - \omega_a), \quad (7)$$

$$J_{ij} = - \sum_{\lambda} g_{\lambda i} g_{\lambda j} e^{i\vec{k} \cdot \vec{r}_{ij}} \text{P} \left(\frac{1}{\omega_{\lambda} - \omega_a} \right), \quad (8)$$

where $\vec{r}_{ij} = \vec{r}_i - \vec{r}_j$ and P stands for the principal part as usual. The Lamb shift δ_L simply leads to a redefinition of the atomic resonant frequency and hereafter we simply ignore it. Clearly, $1/T_2$ and γ_{ij} are proportional to the density of states at the atomic resonant frequency ω_a . Deep inside the gap where the density of modes is very small, $1/T_2$ and γ_{ij} are negligible. In the case when additional homogeneous broadening is present, T_1 and T_2 may be considered as empirical constants. While $1/T_2$ and γ_{ij} are very small inside the gap, the dipole-dipole interaction (RDDI) J_{ij} may behave differently because of the exchange of virtual photons. For an isotropic PBG [$\omega_{\lambda} \equiv \omega_k = \omega(k)$] after converting the mode sum over transverse plane waves into an integral and performing the angular integral, Eq. (8) can be written as [14,17,23]

$$J_{ij} = - \frac{\mu^2 \omega_a^2}{4 \pi^2 \epsilon_0 \hbar} \int_0^{\infty} \frac{k^2}{\omega_k} \tau(k r_{ij}) \text{P} \left(\frac{1}{\omega_k - \omega_a} \right) dk. \quad (9)$$

Here

$$\tau(x) = \alpha \frac{\sin x}{x} + \beta \left(\frac{\sin x}{x^3} - \frac{\cos x}{x^2} \right), \quad (10)$$

where

$$\begin{cases} \alpha = 0, \beta = 2 & \text{for } \Delta m = 0 \text{ transition} \\ \alpha = 1, \beta = -1 & \text{for } \Delta m = \pm 1 \text{ transition,} \end{cases} \quad (11)$$

$r_{ij} = |\vec{r}_{ij}|$, and $k = |\vec{k}|$. The numerical simulations of J_{ij} as a function of r_{ij} for typical isotropic PBG dispersion relations $\omega(k)$ were conducted in Refs. [14,17], where it has been shown that J_{ij} approaches its free space value for atomic distances much smaller than the optical wavelength. For atomic distances larger than the localization length, the RDDI becomes negligible [14].

In analogy to the free space case [19,20], we factorize the products of the dipole operators among different atoms (mean-field approximation). We also ignore the small parameter γ_{ij} which depends on the minute density of states inside the gap and rewrite Eqs. (3) and (4) in the form

$$\begin{aligned} \frac{d}{dt} \langle \sigma_i \rangle &= (-1/T_2 + i\delta) \langle \sigma_i \rangle - i\Omega e^{i\vec{k}_0 \cdot \vec{r}_i} \langle \sigma_i^z \rangle \\ &+ i \sum_{j(\neq i)} J_{ij} \langle \sigma_i^z \rangle \langle \sigma_j \rangle, \end{aligned} \quad (12)$$

$$\begin{aligned} \frac{d}{dt} \langle \sigma_i^z \rangle &= -(\langle \sigma_i^z \rangle + 1)/T_1 + 2i\Omega (\langle \sigma_i^+ \rangle e^{i\vec{k}_0 \cdot \vec{r}_i} - \langle \sigma_i \rangle^{-i\vec{k}_0 \cdot \vec{r}_i}) \\ &- 2i \sum_{j(\neq i)} J_{ij} [\langle \sigma_i^+ \rangle \langle \sigma_j \rangle - \langle \sigma_j^+ \rangle \langle \sigma_i \rangle]. \end{aligned} \quad (13)$$

Analogous equations have been derived previously [13,18] using the effective Hamiltonian

$$\begin{aligned} H_{\text{eff}} &= -\frac{\hbar}{2} \delta \sum_i \sigma_i^z - \hbar \Omega \sum_i (\sigma_i e^{-i\vec{k}_0 \cdot \vec{r}_i} + \sigma_i^+ e^{i\vec{k}_0 \cdot \vec{r}_i}) \\ &+ \sum_{ij} J_{ij} \sigma_i^+ \sigma_j, \end{aligned} \quad (14)$$

in which the decay rates $1/T_1$ and $1/T_2$ were introduced phenomenologically.

III. NONLINEAR ATOMIC RESPONSE

In this section we derive a general expression for the nonlinear susceptibility of two-level atoms in a PBG from the applied field. For simplicity we assume that the atoms are located in a volume with dimension smaller than the resonant wavelength $\lambda_0 = 2\pi c/\omega_a$, leading to the simplification $e^{-i\vec{k}_0 \cdot \vec{r}_{ij}} \approx 1$. Equations (12) and (13) then become

$$\begin{aligned} \frac{d}{dt} \langle \sigma_i \rangle &= (-1/T_2 + i\delta) \langle \sigma_i \rangle - i\Omega \langle \sigma_i^z \rangle \\ &+ J_0 \langle \sigma_i^z \rangle \sum_{j(\neq i)} \langle \sigma_j \rangle + i \langle \sigma_i^z \rangle F_i, \end{aligned} \quad (15)$$

$$\begin{aligned} \frac{d}{dt} \langle \sigma_i^z \rangle &= -(\langle \sigma_i^z \rangle + 1)/T_1 + 2i\Omega (\langle \sigma_i^+ \rangle - \langle \sigma_i \rangle) \\ &- 2iJ_0 \left(\langle \sigma_i^+ \rangle \sum_{j(\neq i)} \langle \sigma_j \rangle - \langle \sigma_i \rangle \sum_{j(\neq i)} \langle \sigma_j^+ \rangle \right) \\ &- 2i \langle \sigma_i^+ \rangle F_i + 2i \langle \sigma_i \rangle F_i^*. \end{aligned} \quad (16)$$

Here,

$$J_{ij} = J_0 + \tilde{J}_{ij} \quad (17)$$

and

$$F_i = \sum_{j(\neq i)} \tilde{J}_{ij} \langle \sigma_j \rangle. \quad (18)$$

$J_0 = [J_{ij}]_c$ is the average value of the RDDI over the random atomic configurations and $\tilde{J}_{ij} = J_{ij} - J_0$ is the fluctuation about this average. A nonzero average J_0 arises in our two-level atom model, when the atomic density is large. If the average interatomic spacing is much smaller than the optical wavelength, the oscillatory spatial behavior of J_{ij} is not important. If the excited state of the atom is a triply degenerate p level, the function $\tau(x)$ in the equation must be replaced [14] by a Cartesian tensor $\tau_{m,n}(x)$, in which the coefficient α is replaced by the transverse tensor $(\delta_{mn} - \hat{r}_{ij}^m \hat{r}_{ij}^n)$ and the coefficient β is replaced by the traceless tensor $(\delta_{mn} - 3\hat{r}_{ij}^m \hat{r}_{ij}^n)$. Here, \hat{r}_{ij}^m is the m component of the unit vector $\hat{r}_{ij} \equiv \vec{r}_{ij}/|\vec{r}_{ij}|$. Deep inside a PBG, the localization length is comparable to the optical wavelength, and the traceless part of RDDI is dominant. This is analogous to choosing $J_0 = 0$ in the two-level atom (scalar) model of RDDI. Closer to the photonic band edges, the localization length becomes much longer than the optical wavelength. In this case, the transverse part of RDDI becomes comparatively important. This is analogous to choosing J_0 to be nonzero in the scalar model. Replacing $\sum_{j(\neq i)} \langle \sigma_j \rangle$ in Eqs. (15) and (16) by its configuration averaged value $N \langle \sigma_i \rangle$, we have

$$\begin{aligned} \frac{d}{dt} \langle \sigma_i \rangle &= (-1/T_2 + i\delta) \langle \sigma_i \rangle - i\Omega \langle \sigma_i^z \rangle + i\tilde{J}_0 \langle \sigma_i^z \rangle \langle \sigma_i \rangle \\ &+ i \langle \sigma_i^z \rangle F_i, \end{aligned} \quad (19)$$

$$\begin{aligned} \frac{d}{dt} \langle \sigma_i^z \rangle &= -(\langle \sigma_i^z \rangle + 1)/T_1 + 2i\Omega (\langle \sigma_i^+ \rangle - \langle \sigma_i \rangle) - 2i \langle \sigma_i^+ \rangle F_i \\ &+ 2i \langle \sigma_i \rangle F_i^*, \end{aligned} \quad (20)$$

where $\tilde{J}_0 = J_0 N$. If we ignore the fluctuation of RDDI, i.e., setting $F_i = F_i^* = 0$, Eqs. (19) and (20) reduce to those of earlier treatments [19] describing atoms in free space. The detailed microscopic evaluation of J_{ij} in an isotropic PBG may be found in Refs. [14,17]. Here, for simplicity, we assume that $\tilde{J}_{ij} = J_{ij} - J_0$ is a Gaussian random number with zero mean value and with variance J . It is straightforward to show that the steady-state solutions of Eqs. (19) and (20) satisfy the conditions

$$w_i^2 + w_i + 4(T_1/T_2)|p_i|^2 = 0 \quad (21)$$

and

$$-\Omega w_i + (\delta + \tilde{J}_0 w_i + i/T_2) p_i + w_i \sum_{j(\neq i)} \tilde{J}_{ij} p_j = 0. \quad (22)$$

Here $p_i \equiv \langle \sigma_i \rangle_s$ and $w_i \equiv \langle \sigma_i^z \rangle_s$ are steady-state expectation values. It is clear from Eq. (21) that the population difference w_i is negative for all atoms and is not directly driven by random fluctuations of \tilde{J}_{ij} . On the other hand, random fluctuations in RDDI drive phase changes in the atomic dipoles, p_i . These phase fluctuations dominate the system behavior in the long time limit. That is, the configuration fluctuations of the population difference are much smaller than the phase fluctuations and can be ignored: ($[w_i^2]_c \cong [w_i]_c^2$). We have performed detailed numerical simulations of Eqs. (21) and (22) for a small number of atoms which confirm this picture. Below, we focus only on the analytical calculation. Configuration averaging over the random atomic positions corresponds to performing a statistical average over the possible values of \tilde{J}_{ij} using the Gaussian distribution. It is denoted by the square brackets $[\]_c$. Ignoring the fluctuations of w_i (mean-field approximation), we can write Eq. (21) as

$$w^2 + w + 4(T_1/T_2)q = 0. \quad (23)$$

Here, $q \equiv (1/N) \sum_i^n [p_i^2]_c$ is the Edwards-Anderson spin-glass order parameter [24,25] and $w \equiv (1/N) \sum_i^n [w_i]_c$ is the average atomic population difference. Mean-field theory has also been applied to Eq. (22) by replacing w_i by its average value w . Equation (22) then becomes

$$-\Omega w + (\delta + \tilde{J}_0 w + i/T_2) p_i + w \sum_{j(\neq i)} \tilde{J}_{ij} p_j = 0. \quad (24)$$

Using the spectral representation of the symmetric matrix ($\tilde{J}_{ij} = \tilde{J}_{ji}$)

$$\tilde{J}_{ij} = \sum_{\lambda=1}^N \langle i|\lambda\rangle \langle \lambda|j\rangle, \quad (25)$$

where J_λ and $\langle \lambda|i\rangle$ are the eigenvalues and orthonormal eigenvectors of \tilde{J}_{ij} , respectively. The polarization eigenmode, $p_\lambda \equiv \sum_j \langle \lambda|j\rangle p_j$, can then be found in the form

$$p_\lambda = \Omega w \frac{\sum_j \langle \lambda|j\rangle}{\delta + i\gamma_\perp + \tilde{J}_0 w + wJ_\lambda}. \quad (26)$$

This yields

$$p_i = \Omega w \sum_{j,\lambda} \frac{\langle i|\lambda\rangle \langle \lambda|j\rangle}{\delta + i\gamma_\perp + \tilde{J}_0 w + wJ_\lambda}. \quad (27)$$

In the limit of large N , the eigenvalue density $\rho(J_\lambda)$ obeys a semicircular law [26,27]

$$\rho(J_\lambda) = \frac{1}{2\pi\tilde{J}^2} (4\tilde{J}^2 - J_\lambda^2)^{1/2}, \quad (28)$$

where $\tilde{J} = J\sqrt{N}$. Using Eq. (28) it is straightforward to determine the average atomic polarization $p = (1/N) \sum_j [p_j]_c$:

$$p = \frac{w\Omega}{2\pi\tilde{J}^2} \int_{-2\tilde{J}}^{2\tilde{J}} (4\tilde{J}^2 - J_\lambda^2)^{1/2} \frac{dJ_\lambda}{\delta + i/T_2 + \tilde{J}_0 w + wJ_\lambda}. \quad (29)$$

Here the off-diagonal elements $[\langle i|\lambda\rangle \langle \lambda|j\rangle]_c$ with $i \neq j$ have been ignored [18,26].

In a similar manner, the spin-glass order parameter can be found as

$$\begin{aligned} q &= \frac{1}{N} \sum_j [p_j^2]_c = \frac{1}{N} \sum_\lambda [p_\lambda^2]_c \\ &= -T_2 \Omega^2 w^2 \text{Im} \int_{-2\tilde{J}}^{2\tilde{J}} (4\tilde{J}^2 - J_\lambda^2)^{1/2} \frac{dJ_\lambda}{\delta + i/T_2 + \tilde{J}_0 w + wJ_\lambda}. \end{aligned} \quad (30)$$

The susceptibility per atom can be defined as $\chi = p/\Omega$.

$$\chi = \frac{1}{2w\tilde{J}^2} \{ \delta + \tilde{J}_0 w + i/T_2 - [(\delta + \tilde{J}_0 w + i/T_2)^2 - 4w^2\tilde{J}^2]^{1/2} \}. \quad (31)$$

For comparison we introduce the scaled spin-glass order parameter $q_\Omega \equiv q/\Omega^2$, which can be related to the susceptibility through Eqs. (29) and (30):

$$q_\Omega = -T_2 w \chi''. \quad (32)$$

Here $\chi = \chi' + i\chi''$, and χ' and χ'' are the real and imaginary parts of the atomic susceptibility χ . Putting Eq. (32) into Eq. (23) we have

$$w = I\chi'' - 1, \quad (33)$$

where $I \equiv 4T_1\Omega^2$ is a scaled intensity parameter. Equations (31)–(33) are the main results of this section. In the case of $\tilde{J}, \tilde{J}_0 \ll 1/T_2$, Eq. (31) reduces to the result of the conventional nonlinear susceptibility [28]:

$$\chi = -(\delta - i/T_2) / [\delta^2 + 1/T_2^2 + 4T_1\Omega^2/T_2]. \quad (34)$$

The conventional nonlinear susceptibility (34) exhibits saturation in *both* the real and imaginary parts. A second limiting case may be recaptured for weak applied field $I \ll 1$. Here, $w \cong -1$ and the linear susceptibility is written as

$$\chi_L = -\frac{1}{2\tilde{J}^2} \{ \delta - \tilde{J}_0 + i/T_2 - [(\delta - \tilde{J}_0 + i/T_2)^2 - 4\tilde{J}^2]^{1/2} \}. \quad (35)$$

In particular, for the case of $\tilde{J} \ll 1/T_2$ the linear susceptibility reduces to

$$\chi_L = -\frac{1}{\delta - \tilde{J}_0 + i/T_2}. \quad (36)$$

It is apparent from Eqs. (35) and (36) that when the mean value of RDDI is nonzero, the resonant frequency shifts to $\omega = \omega_a - \tilde{J}_0$. The value $-\tilde{J}_0$ is called the ‘‘blue’’ or ‘‘red’’ shift depending on whether \tilde{J}_0 is negative or positive. The magnitude of this shift depends on the density of the atomic

medium and has been discussed extensively as a means to obtain information about the spatial, coherent properties of distant objects [29,30].

In the case of large \tilde{J} , the saturation effect described by Eq. (34) is modified dramatically. In particular, we have shown [31] that although strong nonlinear suppression of absorption occurs, the (real) nonlinear index of refraction remains large in a certain domain of applied field intensity. This occurs due to the formation of a glassy state of the atomic dipoles. Although optical absorption to these dipoles has been saturated, they remain highly polarizable due to their random phases. In this paper we examine the nonequilibrium phase transitions which occur among these dipoles as a function of the applied field, using the general susceptibility equation (31).

IV. SECOND-ORDER PHASE TRANSITION AND THE OPTICAL SPIN-GLASS STATE

The equilibrium second-order phase transition for disordered spin systems has been discussed extensively in the context of spin glasses [24,25]. For two-level atoms with a transition in the optical domain the role of thermal fluctuation is unimportant. We focus instead on the nonequilibrium phase transition, induced by the external field, from a spin-glass state to a ferroelectric state. For simplicity we assume in this section that $J_0 \cong 0$ and the decay rates $1/T_1$, $1/T_2$ are much smaller than the variance \tilde{J} of RDDI between atoms. As discussed earlier, the assumption $J_0 \cong 0$ can be satisfied deep inside the PBG in a realistic description when the RDDI in Eq. (9) is replaced by a traceless tensor interaction for atomic transitions between degenerate atomic states. The susceptibility in Eq. (31) becomes imaginary ($\chi' = 0$) at the exact resonance $\delta = 0$ and has the form

$$\chi'' = [(1 + 4w^2 T_2^2 \tilde{J}^2)^{1/2} - 1] / (2|w| T_2 \tilde{J}^2). \quad (37)$$

It is instructive to consider the relative importance of glassy configurations which are measured by the ratio of the ferroelectric to the ferroglass order parameter.

$$\chi_q \equiv \frac{|\chi|^2}{q\Omega} = [(1 + 4w^2 T_2^2 \tilde{J}^2)^{1/2} - 1] / (2w^2 T_2^2 \tilde{J}^2). \quad (38)$$

Clearly for $\tilde{J} \gg 1/T_2$, and for sufficiently weak applied field that the atomic population difference $w \cong -1$, we have $\chi_q \cong 1/(T_2 \tilde{J}) \ll 1$. That is, the glassy behavior of the atomic dipoles becomes dominant relative to any macroscopic ferroelectric response. For the strong applied field, the atomic system tends to be saturated with $w \cong 0$. In this case $\chi_q \cong 1$, i.e., the ferroelectric behavior becomes dominant. With the help of Eqs. (33) and (37) we can write the equation for the atomic difference w and for χ'' as

$$w^3 + 2w^2 + w \left(1 - \frac{I}{T_2 \tilde{J}^2} - \frac{I^2}{\tilde{J}^2} \right) - \frac{I}{T_2 \tilde{J}^2} = 0 \quad (39)$$

and $\chi'' = (w + 1)/I$. Using the solution of Eq. (39) we can easily find w , χ'' , and χ_q in the limit of $\tilde{J} \gg 1/T_2$ as

$$w \cong \begin{cases} I/\tilde{J} - 1 & \text{for } I \leq \tilde{J} \\ 0 & \text{if } I > \tilde{J}, \end{cases} \quad (40)$$

$$\chi'' \cong \begin{cases} 1/\tilde{J} & \text{if } I \leq \tilde{J} \\ 1/I & \text{if } I > \tilde{J}, \end{cases} \quad (41)$$

$$\chi_q \cong \begin{cases} 0 & \text{if } I \leq \tilde{J} \\ 1 - \tilde{J}^2/I^2 & \text{if } I > \tilde{J}. \end{cases} \quad (42)$$

Equations (40)–(42) show clearly the second-order nonequilibrium phase transition in atomic population difference, absorption coefficient χ'' , and in χ_q at $I = \tilde{J}$. In particular, the phase transition from spin-glass state with $\chi_q \cong 0$ to ferroelectric state occurs. For finite values of $1/(T_2 \tilde{J})$, this transition is smeared and there is no slope discontinuity in the response function χ or the order parameter w . Unlike the conventional phase transition described in spin-glass literature [24,25], our phase transition occurs at $w \cong 0$. That is, the atomic system is far from equilibrium. The second-order phase transition is also shown in Fig. 1 as a result of the numerical solution of Eqs. (33), (37), and (38) for the case of $\tilde{J} \gg 1/T_2$. This can be easily satisfied in a PBG. This suggests that the quantum-optical spin-glass state may be created and controllably altered by means of an external laser field.

V. OPTICAL BISTABILITY

Optical bistability occurs when there are two stable states for the light intensity transmitted through a nonlinear material for one value of the input intensity I_{in} [32–35]. The transmitted intensity which the output settles down to depends on the excitation history. A different state is reached if one either decreases the incident intensity I_{in} from a sufficiently high original level, or if one increases I_{in} from zero. The possibility to switch a bistable optical device between its two states facilitates the use of such a device as a binary optical memory. The fact that bistable elements can be addressed simultaneously by many laser beams suggests the possibility of parallel optical data processing [34]. Current applied research is focused on optimizing these devices by decreasing their size, switching times, and threshold power.

In this section we discuss optical bistability in the atomic response in PBG materials. Spontaneous emission can be strongly suppressed in a PBG while RDDI displays only small deviation from the free space case for atomic separation smaller than an optical wavelength [14,17]. As a result, RDDI can dominate relaxation rates even at relatively low atomic density. In contrast to the free space case [19], the role of RDDI's fluctuations in optical bistability will be discussed in detail.

For comparison purposes, we begin with the case when the fluctuations in RDDI are ignored, i.e., $\tilde{J} \cong 0$ while $\tilde{J}_0 \neq 0$. In this case it is straightforward to derive a cubic equation for the atomic population difference from Eqs. (31)–(33) in the form

$$\tilde{J}_0^2 w^3 + J_0 (2\delta + \tilde{J}_0) w^2 + (\delta^2 + 1/T_2^2 + 4T_1 \Omega^2 / T_2 + 2\delta \tilde{J}_0) w + 1/T_2^2 + \delta^2 = 0. \quad (43)$$

For $\tilde{J}_0 = 0$, Eq. (43) has a solution

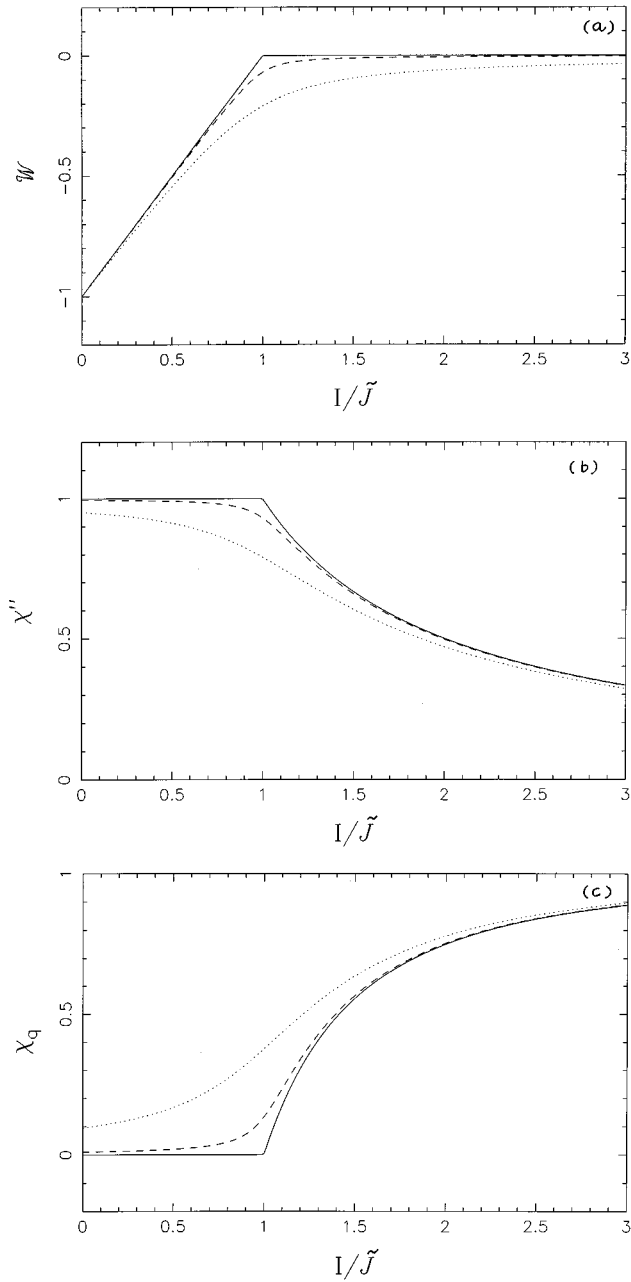


FIG. 1. (a) Atomic population difference w , (b) absorption coefficient χ'' , and (c) χ_q (in units of $\tilde{J}=1$) as a function of I/\tilde{J} for $\delta=\tilde{J}_0=0$ and for $1/(T_2\tilde{J})=10^{-5}$ (solid curves), 0.01 (dashed curves), and 0.1 (dotted curves).

$$w = -(1 + \delta^2 T_2^2) / [1 + \delta^2 T_2^2 + 4T_1 T_2 \Omega^2]. \quad (44)$$

The absorption coefficient χ'' can be found from Eqs. (33) and (44) as

$$\chi'' = T_2 / [1 + \delta^2 T_2^2 + 4T_1 T_2 \Omega^2]. \quad (45)$$

Clearly, as the input applied field intensity Ω^2 increases, the atomic population difference, which is proportional to the output, increases monotonically from the equilibrium value $w = -1$ to the saturation value $w = 0$ at $\Omega \rightarrow \infty$. Analogously, the absorption coefficient decreases monotonically and there is no hysteresis or bistable behavior in the system.

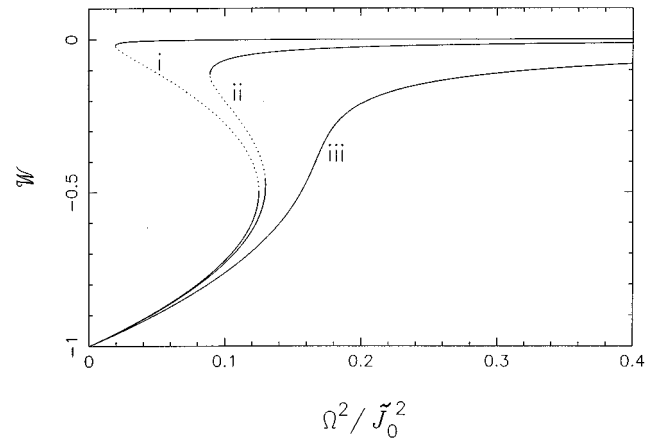


FIG. 2. Atomic population difference w as a function of Ω^2/\tilde{J}_0^2 for $\tilde{J}_0 = -1$, $\delta = \tilde{J} = 0$, and for (i) $1/(T_2|\tilde{J}_0|) = 1/(2T_1|\tilde{J}_0|) = 0.02$, (ii) 0.1, and (iii) 0.25. The solid and dotted curves represent stable and unstable states, respectively.

In the case with $\tilde{J}_0 \neq 0$, the cubic equation (43) may lead to bistability effects. That is, as the field intensity increases and the Rabi frequency becomes large relative to \tilde{J}_0 and $1/T_2$, the two-level system switches suddenly from the low-transmission branch to the high-transmission branch. This bistability behavior is shown in Figs. 2 and 3 where the atomic population difference (Fig. 2) and associated χ'' are plotted as a function of Ω^2 . In Figs. 2 and 3, the solid and dotted curves with positive and negative slopes, respectively, represent stable and unstable states. These plots are obtained by solving the cubic equation (43) as a function of the parameters Ω , T_1 , T_2 , and \tilde{J}_0 . The turning points where the slope is infinity corresponds to points where the roots of the cubic equation undergo a Hopf bifurcation: two complex conjugate roots become two real roots or vice versa. The stability of each solution is determined by doing a stability analysis of the time-dependent Heisenberg equations of motion (19) and (20) (see Appendix B). For the stable solution, a small fluctuation about the steady-state value decreases exponentially whereas for the unstable branch, a small fluctua-

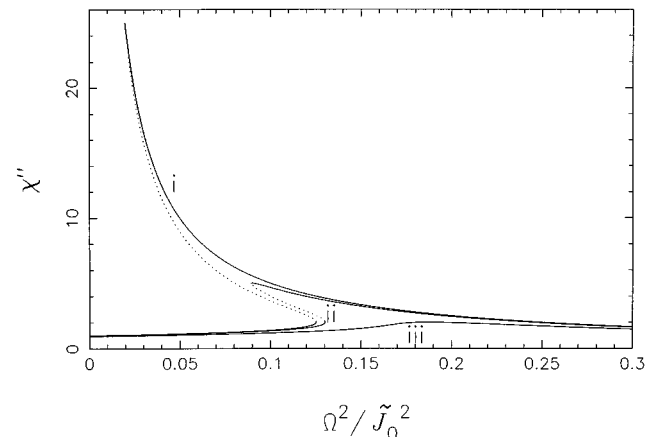


FIG. 3. χ'' as a function of Ω^2/\tilde{J}_0^2 for the same parameters as in Fig. 2.

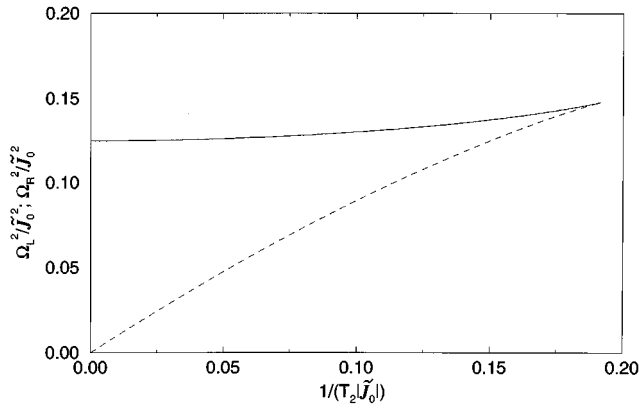


FIG. 4. Threshold applied field intensity at the left Ω_L^2/\tilde{J}_0^2 (dashed curve) and right switching points Ω_R^2/\tilde{J}_0^2 (solid curve) as a function of $1/(T_2|\tilde{J}_0|)$ and for $\delta=J=0$, $T_1=T_2/2$, $\tilde{J}_0=-1$.

tion grows until it reaches one of the two stable solutions nearby [19,33].

Although an exact analytical solution of the cubic equation (43) can be easily found, it does not provide the most transparent picture of the system behavior. However, the turning points (where the roots undergo Hopf bifurcation) for w as a function of Ω can be determined by setting the derivative of the left-hand side of Eq. (43) with respect to w equal to zero. For the exact resonance case ($\delta=0$) we get

$$w^2 + \frac{2}{3}w + \frac{1+4T_1T_2\Omega^2}{3T_2^2\tilde{J}_0^2} = 0. \quad (46)$$

It yields the following necessary condition for bistability:

$$T_2\tilde{J}_0/\sqrt{3} > \sqrt{1+4T_1T_2\Omega^2}. \quad (47)$$

In a PBG, spontaneous emission is strongly suppressed while RDDI remains strong. Under these circumstances, condition (47) can be easily satisfied even for the relatively small atomic density. The threshold applied field intensity at the switching points can be found from Eqs. (43) and (46). In particular, for the case of $\tilde{J}_0 \gg 1/T_2$, the Rabi frequencies at the switching from the low-transmission branch to high-transmission branch (the right turning point), Ω_R , and for the switching from low-transmission branch to high-transmission branch (the left turning point), Ω_L , is given by

$$\Omega_R^2 \cong \tilde{J}_0^2 T_2 / (16T_1), \quad (48)$$

$$\Omega_L^2 \cong 0. \quad (49)$$

This is in very good agreement with Fig. 4 where we plot $(\Omega_L)^2$ and $(\Omega_R)^2$ calculated numerically from Eqs. (43) and (46) as a function of $1/(T_2|\tilde{J}_0|)$. Clearly from Fig. 4, bistability occurs only if

$$\tilde{J}_0 T_2 \leq 0.19. \quad (50)$$

In a PBG, where T_2 is of many orders of magnitude larger than in free space, the condition (50) can be satisfied at a relatively small value of \tilde{J}_0 . As a result, bistability may oc-

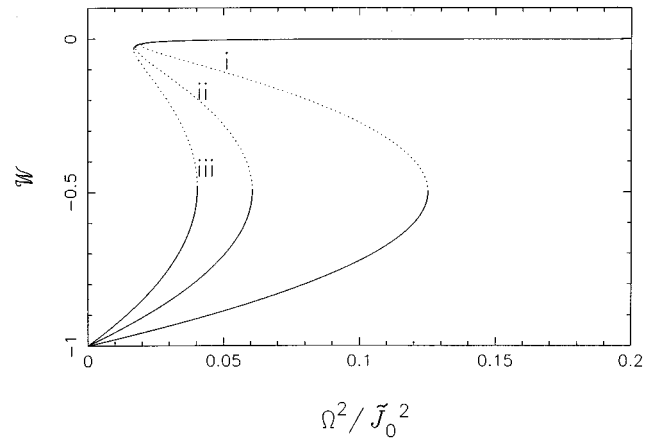


FIG. 5. Atomic population difference w as a function of Ω^2/\tilde{J}_0^2 for $\tilde{J}_0=-1$, $\delta=0$, $1/(T_2|\tilde{J}_0|)=1/(2T_1|\tilde{J}_0|)=0.02$, and for (i) $\tilde{J}/\tilde{J}_0=0$, (ii) 0.4, and (iii) 0.45. The solid and dotted curves represent stable and unstable states, respectively.

cur at a threshold field intensity (48) much smaller than that required in free space [19,35].

To recover the effects of RDDI fluctuations on bistability, we numerically evaluate the general expression for susceptibility given in Eqs. (31) and (33). In Fig. 5 we plot the atomic population difference w as a function of Ω^2 for different values of the RDDI variance \tilde{J} . It is clear that very strong fluctuation of RDDI reduces bistability effects. However, it is interesting to note here that the increase of \tilde{J} leads to a reduction of the threshold intensity for switching from the low-transmission branch to the high-transmission branch. This is clearly seen in Fig. 6, in which we plot the switching intensities $(\Omega_L)^2$ and $(\Omega_R)^2$ calculated numerically from Eqs. (31) and (33) as a function of $\tilde{J}/|\tilde{J}_0|$ for different values of $1/(T_2|\tilde{J}_0|)$. At the same time, the decrease of $1/T_2$ leads to a decrease of the threshold energy for switching from the high-transmission branch to the low-transmission branch (see Figs. 4 and 6). This means that in the case $1/T_2 \ll \tilde{J} \sim \tilde{J}_0$, both threshold energies for low-high and high-low switching can

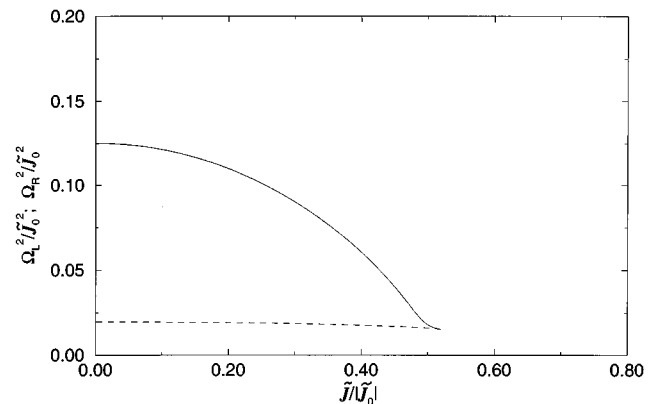


FIG. 6. Threshold applied field intensity at the left Ω_L^2/\tilde{J}_0^2 (dashed curve) and right switching points Ω_R^2/\tilde{J}_0^2 (solid curve) as a function of $\tilde{J}/|\tilde{J}_0|$ for $\delta=0$, $\tilde{J}_0=-1$, and for $1/(T_2|\tilde{J}_0|)=1/(2T_1|\tilde{J}_0|)=0.02$.

be many orders of magnitude smaller than in free space and these thresholds can be controlled by changing the parameters of the PBG system. The magnitude of \tilde{J}/\tilde{J}_0 can be adjusted by varying the atomic density: Since $\tilde{J}_0 = NJ_0$ and $\tilde{J} = \sqrt{N}J$, for a singlet atomic transition, the condition $\tilde{J}_0 \gg \tilde{J}$ can be satisfied by increasing the density of the impurity atoms. In this case the bistability effect (first-order phase transition) will prevail over the second-order phase transition discussed in the preceding section. In a less dense medium and for a triplet atomic transition, \tilde{J} may be much larger than \tilde{J}_0 . In this case, the second-order phase transition and formation of an optical spin-glass state is expected.

VI. CONCLUSION

We have discussed first- and second-order nonequilibrium phase transitions in the response of two-level impurity atoms in an imperfect PBG to an external laser field. The atomic resonant frequency is assumed to lie far from the band edge so that the non-Markovian effects caused by the singularity of density of modes at the band edge can be ignored. We derived the general expression for atomic susceptibility and have shown that in the case when the variance of the RDDI fluctuations is much larger than its average value and atomic relaxation rates, a second-order phase transition occurs at the threshold intensity defined by the variance of RDDI. At this threshold, the system changes from a glassy phase into a ferroelectric phase. In the opposite case when the average value of RDDI is larger than its variance, the phase transition is first order and the system exhibits optical bistability. The bistability in a PBG has been shown to occur at much lower threshold intensity than in free space. The results we have presented have focused on a small active region within a PBG in which N atoms are confined to a volume given by a cubic wavelength. It would be of considerable interest to extend these results into a large active region, in which the impurity atoms are distributed over many optical wavelengths. The spatial and temporal evolution of the coupled atom plus optical field, however, requires that we generalize the optical Bloch equations [20] to a set of coupled Maxwell-Bloch equations appropriate for a PBG.

ACKNOWLEDGMENTS

This work was supported in part by the Natural Sciences and Engineering Research Council of Canada and the Ontario Laser and Lightwave Research Centre.

APPENDIX A

In this appendix we will derive the general (non-Markov) optical Bloch equation. The Heisenberg equations of motion can be derived from the Hamiltonian (1) as

$$\frac{d}{dt} a_\lambda = -i\delta_\lambda a_\lambda + \sum_i g_{\lambda i} e^{-i\vec{k}\cdot\vec{r}_i} \sigma_i, \quad (\text{A1})$$

$$\frac{d}{dt} \sigma_i = i\delta\sigma_i + \sum_\lambda g_{\lambda i} e^{i\vec{k}\cdot\vec{r}_i} \sigma_i^\dagger a_\lambda - i\Omega e^{i\vec{k}_0\cdot\vec{r}_i} \sigma_i^z, \quad (\text{A2})$$

$$\begin{aligned} \frac{d}{dt} \sigma_i^z &= 2i\Omega (\sigma_i^+ e^{i\vec{k}_0\cdot\vec{r}_i} - \sigma_i^- e^{-i\vec{k}_0\cdot\vec{r}_i}) \\ &\quad - 2 \sum_\lambda g_{\lambda i} (\sigma_i^+ a_\lambda e^{i\vec{k}\cdot\vec{r}_i} + a_\lambda^+ \sigma_i^- e^{-i\vec{k}\cdot\vec{r}_i}). \end{aligned} \quad (\text{A3})$$

The formal solution of Eq. (A1) has the form

$$a_\lambda(t) = e^{-i\delta_\lambda t} a_\lambda(0) + \sum_i g_{\lambda i} \int_0^t e^{-i[\vec{k}\cdot\vec{r}_i + \delta_\lambda(t-t')]} \sigma_i(t') dt'. \quad (\text{A4})$$

Putting $a_\lambda(t)$ into Eqs. (A2) and (A3) we obtain the equations for quantum expectation values in the form

$$\begin{aligned} \frac{d}{dt} \langle \sigma_i(t) \rangle &= i\delta \langle \sigma_i(t) \rangle - i\Omega e^{i\vec{k}_0\cdot\vec{r}_i} \langle \sigma_i^z(t) \rangle \\ &\quad + \int_0^t G_{ii}(t-t') \langle \sigma_i^z(t) \sigma_i(t') \rangle dt' \\ &\quad + \sum_{j(\neq i)} \int_0^t G_{ij}(t-t') \langle \sigma_i^z(t) \sigma_j(t') \rangle dt', \end{aligned} \quad (\text{A5})$$

$$\begin{aligned} \frac{d}{dt} \langle \sigma_i^z(t) \rangle &= 2i\Omega [e^{i\vec{k}_0\cdot\vec{r}_i} \langle \sigma_i^+(t) \rangle - e^{-i\vec{k}_0\cdot\vec{r}_i} \langle \sigma_i(t) \rangle] \\ &\quad - 2 \int_0^t dt' G_{ii}(t-t') \langle \sigma_i^+(t) \sigma_i(t') \rangle \\ &\quad - 2 \int_0^t dt' G_{ii}^*(t-t') \langle \sigma_i^+(t') \sigma_i(t) \rangle \\ &\quad - 2 \sum_{j(\neq i)} \int_0^t dt' G_{ij}(t-t') \langle \sigma_i^+(t) \sigma_j(t') \rangle \\ &\quad - 2 \sum_{j(\neq i)} \int_0^t dt' G_{ij}^*(t-t') \langle \sigma_j^+(t') \sigma_i(t) \rangle, \end{aligned} \quad (\text{A6})$$

where

$$G_{ii}(t-t') = \sum_\lambda g_{\lambda i}^2 e^{-i\delta_\lambda(t-t')}, \quad (\text{A7})$$

$$G_{ij}(t-t') = \sum_\lambda g_{\lambda i} g_{\lambda j} e^{i\vec{k}\cdot\vec{r}_{ij} - i\delta_\lambda(t-t')}. \quad (\text{A8})$$

Here $\vec{r}_{ij} = \vec{r}_i - \vec{r}_j$.

$G_{ii}(t-t')$ and $G_{ij}(t-t')$ are delay Green's functions and their implicit form strongly depends on the dispersion relation $\omega_{\vec{k}} = \omega(\vec{k})$. For example, at the edge of the isotropic PBG, the Green function $G_{ii}(t-t') \sim (t-t')^{-1/2}$ [12]; rather than $G_{ii}(t-t') \sim \delta(t-t')$ as in a free space, this leads to non-Markov phenomena in spontaneous emission [11] and superradiance [12]. The calculation of the Green's function $G_{ij}(t-t')$ at the edge of a PBG and a study of non-Markov effects on the phase transitions near the band edge goes beyond the scope of this paper and we plan to present them

elsewhere. In this paper we have considered only the case when the atomic resonant frequency lies deep in the pseudogap where the density of modes does not change considerably. In such a case, the memory effects caused by the irregularity in the density of states at the edges of a PBG can be ignored (Markov approximation). More specifically, t' in two-time correlation functions in Eqs. (A5) and (A6) are replaced by t and the correlation functions can then be taken out of the integral. The integrals $\int_0^t G_{ii}(t') dt'$ and $\int_0^t G_{ij}(t') dt'$ can be calculated easily as for the free space case [36] and Eqs. (A5) and (A6) can be written in the form of Eqs. (3) and (4).

APPENDIX B

In this appendix we give a linear stability analysis for the solutions of Eq. (43). For simplicity we consider only the case of exact resonance $\delta=0$. Ignoring the fluctuation of RDDI, i.e., setting $F_i = F_i^* = 0$, Eqs. (19) and (20) become

$$\frac{d}{dt} \langle \sigma \rangle = -\langle \sigma \rangle / T_2 + i\tilde{J}_0 \langle \sigma^z \rangle \langle \sigma \rangle - i\Omega \langle \sigma^z \rangle, \quad (\text{B1})$$

$$\frac{d}{dt} \langle \sigma^z \rangle = -(\langle \sigma^z \rangle + 1) / T_1 + 2i\Omega (\langle \sigma^\dagger \rangle - \langle \sigma \rangle), \quad (\text{B2})$$

and $(d/dt) \langle \sigma^\dagger \rangle = [(d/dt) \langle \sigma \rangle]^*$. For infinitesimal perturbations of the system from the steady state

$$\langle \sigma \rangle = p + \delta p, \quad \langle \sigma^\dagger \rangle = p^* + \delta p^*, \quad \langle \sigma^z \rangle = w + \delta w, \quad (\text{B3})$$

where p and w are the steady-state values of the atomic polarization and population inversion. Neglecting the nonlinear terms of δp and δw we find equations of motion for δp and δw from Eqs. (B1) and (B2) as

$$\frac{d}{dt} \delta p = -\frac{\delta p}{T_2} + i\tilde{J}_0 p \delta w + i\tilde{J}_0 w \delta p - i\Omega \delta w, \quad (\text{B4})$$

$$\frac{d}{dt} \delta w = -\frac{\delta w}{T_1} + 2i\Omega \delta p^* - 2i\Omega \delta p, \quad (\text{B5})$$

and $(d/dt) \delta p^* = [(d/dt) \delta p]^*$. The eigenvalue equation for Eqs. (B4) and (B5) can be written as

$$\begin{vmatrix} \Lambda + \frac{1}{T_2} - i\tilde{J}_0 w & 0 & i\Omega - i\tilde{J}_0 p \\ 0 & \Lambda + \frac{1}{T_2} + i\tilde{J}_0 w & -i\Omega + i\tilde{J}_0 p^* \\ 2i\Omega & -2i\Omega & \Lambda + \frac{1}{T_1} \end{vmatrix} = 0. \quad (\text{B6})$$

The relation between p and w can be found from Eq. (B1) as

$$p = \frac{\Omega T_2 w}{T_2 \tilde{J}_0 w + i} = \Omega (\chi' + i\chi''). \quad (\text{B7})$$

With the help of Eqs. (B7) and (33), the eigenvalue equation (B6) can be written as

$$\Lambda^3 + a_1 \Lambda^2 + a_2 \Lambda + a_3 = 0, \quad (\text{B8})$$

where

$$a_1 = \frac{2}{T_2} + \frac{1}{T_1}, \quad (\text{B9})$$

$$a_2 = \frac{2}{T_1 T_2} + \frac{1}{T_2^2} + \tilde{J}_0^2 w^2 + \frac{4\Omega^2}{1 + T_2^2 \tilde{J}_0^2 w^2}, \quad (\text{B10})$$

$$a_3 = \frac{\tilde{J}_0^2}{T_1} \left(3w^2 + 2w + \frac{1 + 4T_1 T_2 \Omega^2}{T_2^2 \tilde{J}_0^2} \right). \quad (\text{B11})$$

The system is stable if a small fluctuation about the steady-state value decreases exponentially. That is, the real part of all the eigenvalues Λ must be negative. According to the Routh-Hurwitz criterion [37], the condition for all negative real parts of eigenvalues and the condition of the system stability is $a_i > 0$ ($i=1,2,3$) (Lienard-Chipart test). Clearly, a_1 and a_2 are positive values and the condition of the system stability is $a_3 > 0$. It is straightforward to show from Eq. (43) that

$$\frac{dw}{d\Omega^2} = \frac{4T_1 |w|}{T_2 \tilde{J}_0^2} \left[3w^2 + 2w + \frac{1 + 4T_1 T_2 \Omega^2}{T_2^2 \tilde{J}_0^2} \right] = \frac{4|w|}{T_2} \frac{1}{a_3}. \quad (\text{B12})$$

It is apparent from Eq. (B12) that the turning points are the points where $a_3 = 0$. The solution with the negative slope $dw/d\Omega^2 < 0$ means that $a_3 < 0$. As a result, the state with the negative slope corresponds to the unstable state and is represented by the dotted curves in Figs. 2, 3, and 5.

- [1] S. John, Phys. Rev. Lett. **53**, 2169 (1984); Phys. Rev. B **31**, 304 (1985).
 [2] E. Yablonovitch, Phys. Rev. Lett. **58**, 2059 (1987).
 [3] S. John, Phys. Rev. Lett. **58**, 2486 (1987).
 [4] K. M. Ho, T. J. Chan, and C. M. Soukoulis, Phys. Rev. Lett. **65**, 3152 (1990).
 [5] E. Yablonovitch, T. J. Gmitter, and K. M. Leung, Phys. Rev. Lett. **67**, 2295 (1991).
 [6] For a review of recent progress in the microfabrication of PBG

- materials, see *Photonic Band Gap Materials*, edited by C. M. Soukoulis, Vol. 315 of *NATO Advanced Study Institute, Series E: Applied Sciences* (Kluwer, Dordrecht, 1996).
 [7] E. Ozbay, E. Michel, G. Tuttle, M. Sigala, R. Biswas, and K. M. Ho, Appl. Phys. Lett. **64**, 2059 (1994); E. Ozbay, in *Photonic Band Gap Materials* (Ref. [6]), pp. 41–61.
 [8] C. T. Chan, S. Datta, K. M. Ho, and C. M. Soukoulis, Phys. Rev. B **49**, 1988 (1994).
 [9] S. Fan, P. Villeneuve, R. Meade, and J. Joannopoulos, Appl.

- Phys. Lett. **65**, 1466 (1994); J. D. Joannopoulos, in *Photonic Band Gap Materials* (Ref. [6]), pp. 1–21.
- [10] U. Gruning, V. Lehmann, and C. M. Engelhardt, Appl. Phys. Lett. **66**, 3254 (1995).
- [11] R. F. Nabiev, P. Yeh, and J. J. Sanchez-Mondragon, Phys. Rev. A **47**, 3380 (1993); S. John and Tran Quang, *ibid.* **50**, 1764 (1994).
- [12] S. John and Tran Quang, Phys. Rev. Lett. **74**, 3419 (1995).
- [13] S. John, and Tran Quang, Phys. Rev. A **52**, 4083 (1995).
- [14] S. John and J. Wang, Phys. Rev. Lett. **64**, 2418 (1990); Phys. Rev. B **43**, 12 772 (1991).
- [15] M. Scalora, J. P. Dowling, C. M. Bowden, and M. J. Bloemer, Phys. Rev. Lett. **73**, 1368 (1994).
- [16] S. John, in *Confined Electrons and Photons*, edited by E. Burstein and C. Weisbuch (Plenum, New York, 1995), p. 523; in *Photonic Band Gap Materials* (Ref. [6]), pp. 563–665.
- [17] G. Kweon and N. M. Lawandy, J. Mod. Opt. **41**, 311 (1994).
- [18] S. John and Tran Quang, Phys. Rev. Lett. **76**, 1320 (1996).
- [19] C. M. Bowden and C. C. Sung, Phys. Rev. A **19**, 2392 (1979); Y. Ben-Aryeh, C. M. Bowden, and J. C. Englund, *ibid.* **34**, 3917 (1986).
- [20] R. Inguva and C. M. Bowden, Phys. Rev. A **41**, 1670 (1990).
- [21] E. Yablonovitch and T. J. Gmitter, Phys. Rev. Lett. **63**, 1950 (1989).
- [22] T. W. Mossberg and M. Lewenstein, J. Opt. Soc. Am. B **10**, 340 (1993).
- [23] P. M. Milonni and P. L. Knight, Phys. Rev. A **10**, 1096 (1974); G. S. Agarwal, *Quantum Statistical Theories of Spontaneous Emission* (Springer-Verlag, Berlin, 1974); D. P. Craig and T. Thirunamachandran, *Molecular Quantum Electrodynamics* (Academic, New York, 1984).
- [24] S. F. Edwards and P. W. Anderson, J. Phys. F **5**, 965 (1975).
- [25] D. Sherrington and S. Kirkpatrick, Phys. Rev. Lett. **35**, 1793 (1975); D. Chowdhury, *Spin Glasses and Other Frustrated Systems* (Princeton University Press, Princeton, NJ, 1986).
- [26] J. M. Kosterlitz, D. J. Thouless, and R. C. Jones, Phys. Rev. Lett. **36**, 1218 (1976); W. Kinzel and K. H. Fischer, Solid State Commun. **23**, 68 (1977).
- [27] M. L. Mehta, *Random Matrices* (Academic, New York, 1991); S. F. Edwards and R. C. Jones, J. Phys. A **9**, 1595 (1976).
- [28] A. Yariv, *Quantum Electronics* (Wiley, New York, 1975); R. W. Boyd, *Nonlinear Optics* (Academic, New York, 1992), Chap. 5.
- [29] E. Wolf, Phys. Rev. Lett. **56**, 1370 (1986); G. V. Varada and G. S. Agarwal, Phys. Rev. A **44**, 7626 (1991); D. F. V. James, *ibid.* **47**, 1336 (1993).
- [30] J. J. Maki, M. S. Malcuit, J. E. Sipe, and R. W. Boyd, Phys. Rev. Lett. **67**, 972 (1991).
- [31] S. John and Tran Quang, Phys. Rev. Lett. **76**, 2484 (1996).
- [32] S. L. McCall, H. M. Gibbs, G. G. Churchill, and T. N. C. Venkatesan, Bull. Am. Phys. Soc. **20**, 636 (1975).
- [33] L. A. Lugiato, P. Mandel, and L. M. Narducci, Phys. Rev. A **29**, 1438 (1983); L. A. Lugiato, Prog. Opt. **26**, 69 (1984), and references therein.
- [34] H. M. Gibbs, *Optical Bistability: Controlling Light with Light* (Academic, New York, 1985).
- [35] M. P. Hehlen, H. U. Güdel, Q. Shu, J. Rai, and S. C. Rand, Phys. Rev. Lett. **73**, 1103 (1994).
- [36] L. Allen and J. H. Eberly, *Optical Resonance and Two-Level Atoms* (Wiley, New York, 1975).
- [37] G. A. Korn and T. M. Korn, *Mathematical Handbook for Scientists and Engineers* (McGraw-Hill, New York, 1968), p. 17.